

## BEAM PHYSICS SIMULATION STUDIES OF 70 MeV ISIS INJECTOR LINAC

S. Ahmadiannamin, A. Letchford, S. R. Lawrie, H. V. Cavanagh,  
 ISIS, STFC, Rutherford Appleton Laboratory, Oxfordshire, UK

### Abstract

The ISIS neutron spallation source is a pioneering research infrastructure in the field of high-intensity accelerator physics, catering to scientific users. Comprising a 70 MeV injector linac and an 800 MeV Rapid cycling synchrotron with two beam targets, this facility has witnessed several upgrades in recent years, leading to enhanced transmission efficiency. Further optimization efforts are underway to ensure continuous improvement. This article focuses on beam physics simulation studies conducted on the current ISIS linac, aiming to gain a deeper understanding and analysis of various phenomena observed during routine operations and accelerator physics experimentation. By examining these phenomena, valuable insights can be obtained to inform the future development of high-efficiency injectors for ISIS-II.

### INTRODUCTION

Over nearly 40 years, the ISIS spallation source, based at the Rutherford Appleton Laboratory, has consistently

provided neutrons to scientists worldwide, establishing itself as a pivotal hub for research in the physical and life sciences in UK and Europe.

The accelerator comprises a 70 MeV H<sup>-</sup> injector, an 800 MeV synchrotron, and two target stations. The injector begins with an H<sup>-</sup> ion source, followed by a three-solenoid low-energy beam transport line (LEBT) and a 665 keV, four-rod Radio Frequency Quadrupole (RFQ) operating at 202.5 MHz. A Drift Tube Linac (DTL) consisting of four tanks accelerates the beam to 70 MeV [1, 2].

The layout of each section, including the ion source and RFQ, new Medium Energy Beam Transport (MEBT, to be installed), DTL, and High Energy Drift Space (HEDS), is depicted in Fig. 1.

In recent years, the ISIS machine has undergone several upgrades that have enhanced its reliability and broadened its utility for both users and accelerator physics experiments. [3, 4].

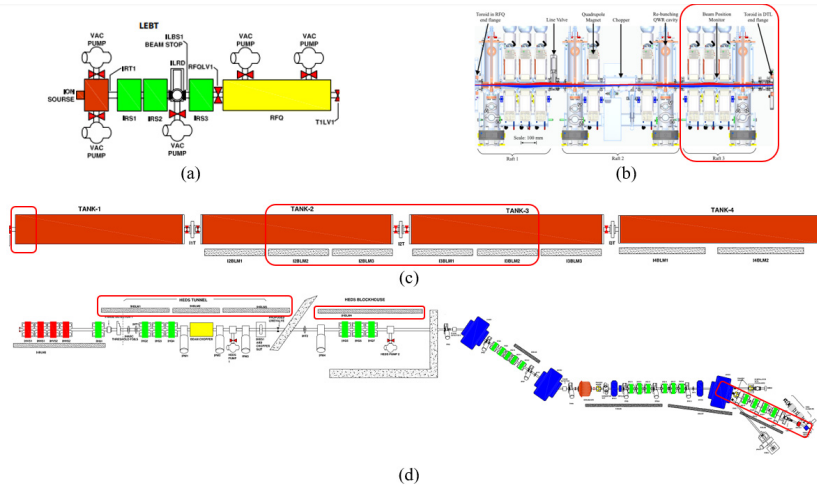


Figure 1: Schematic representation of pre-injector of ISIS (a) ion source, LEBT, RFQ; (b) MEBT design; (c) Drift Tube Linac Tanks, (d) High Energy Drift Section (HEDS) [5, 6].

The parameter settings in each section of the accelerator profoundly impact the transmission efficiency of other sections. It is crucial to view the MEBT, DTL, and HEDS sections as integrated units within the accelerator. This holistic approach enables us to gain a more comprehensive understanding of the events that occur during machine operation, particularly in the areas highlighted with red rectangles in Fig. 1, where non-negligible beam loss is routinely measured. In the subsequent sections the machine's current operational status will be outlined and compared to simulation results before and after implementing the proposed

new MEBT. These simulations were conducted using the Parmila code for beam dynamic simulations [7].

### SIMULATION AND MODELING

The linac comprises four amplifier chains, each consisting of three RF amplifiers, with one chain dedicated to each tank. These amplifier chains comprise a 3-kW solid-state amplifier, a 200-kW tetrode intermediate-power driver stage, and a 2 MW triode high-power output stage. Each of the output stages, delivering approximately 2 MW of power in 400  $\mu$ s pulses. [8].

Content from this work may be used under the terms of the CC-BY-4.0 licence (© 2023). Any distribution of this work must maintain attribution to the author(s), title of the work, publisher, and DOI

In the upcoming sections, we will explore two different configurations of the accelerator injector: with and without the MEBT section.

### (a) ISIS Injector without MEBT

At the current setting of the ISIS linac, the beam parameters at the exit of the RFQ, located approximately 16 cm before the first quadrupole of DTL Tank 1, are as follows [9]:

- Horizontal plane (X-X'):  $\alpha_x = 0.396$ ,  $\beta_x = 0.139$  meters/rad,  $\epsilon_x = \epsilon_{rms-unnorm-x} = 12.8 \pi$ .mm-mrad
- Vertical plane (Y-Y'):  $\alpha_y = -0.531$ ,  $\beta_y = 0.086$  meters/rad,  $\epsilon_y = \epsilon_{rms-unnorm-y} = 12.8 \pi$ .mm-mrad
- Longitudinal plane (W-Phase):  $\alpha_z = 0.045$ ,  $\beta_z = 0.819$  deg/keV,  $\epsilon_z = \epsilon_{rms-unnorm-z} = 120 \pi$ .deg-keV

The beam energy and current at the entrance to the drift and DTL are 0.665 MeV and 35 mA, respectively. Beam halo formation is observed for a gaussian beam in simulations of machine operation. This phenomenon will be studied in more detail in the near future, and different solutions will be considered for mitigation. Fortunately, within the ISIS facility, thanks to the presence of a low-energy injector linac and RCS collimators, the impact of the beam halo on activation due to beam loss remains minimal.

The results of the simulation for current transmission along the Linac and HEDs are shown in Fig. 2 for nominal settings. Also shown are the effect of RF phase and amplitude variations in Tanks 1 – 4, in the order of  $\pm 5$  percent and  $\pm 1$  degree, respectively. As indicated by these simulations, reducing the field amplitude in the tanks has the most significant impact on beam loss, and the magnitude of this impact varies between different tanks. Notably, this impact is particularly pronounced for Tanks 1 and 3.

One of the most effective techniques for improving operations in spallation neutron sources is the active monitoring of beam loss. Besides measuring beam current transmission between different sections of the machine, it is vital that we estimate the power loss per meter to identify the most probable areas for radioactivation and to compare the simulation of beam physics with the machine's operational experiences. In ISIS, this procedure has been in place for a considerable time, and the precise localization of BLMs allows for adjustments to improve transmission while minimizing activation issues. Figure 3 presents simulated beam loss, including the effects of tank RF phase and amplitude variations, on the determination of beam and power loss per unit length of the machine.

Additionally, in Fig. 4, the simulated beam power loss along the Linac during nominal machine operation is depicted. This closely correlates with the measurement results obtained from BLMs along the injector. Notably, a substantial amount of beam power is lost in the first tank of the Linac. Fortunately, due to the low-energy nature of this part, significant activation is not a concern in this case. Depending on machine parameters, approximately 25% to 35% of the beam is lost in the first tank of the machine. Furthermore, we can identify traces of beam loss at the

transitions between linac tanks, with the most significant concentration of loss occurring near HEDS quadrupoles 1, 2, 3, and 4. Also, beam loss occurs at the end of the HEDS, close to injection into the RCS.

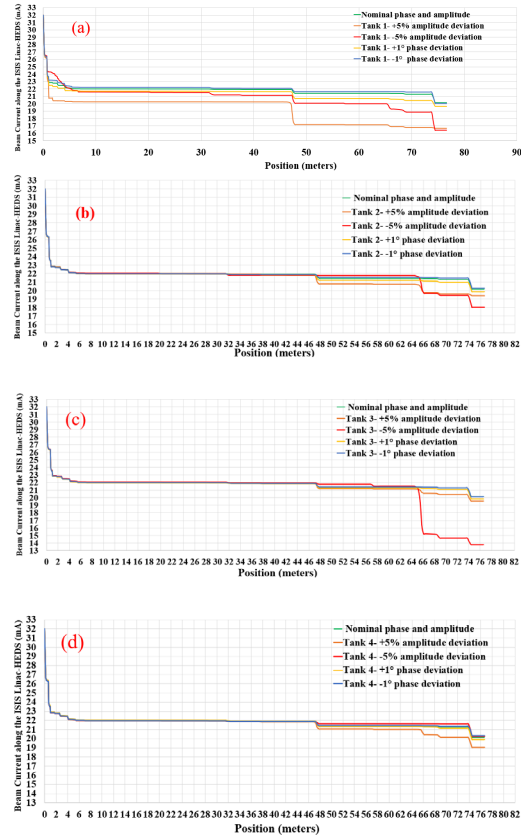


Figure 2: Beam current transmission efficiency in linac and HEDS for RF amplitude and phase deviation in DTL Tanks (a) Tank 1, (b) Tank 2, (c) Tank 3, (d) Tank 4.

The variation in beam energy based on amplitude is not a consistent and predictable occurrence. According to simulation results, when the amplitude of the field in Tanks 1 and 3 is increased, the beam energy also increases compared to the nominal operation of the machine. Conversely, increasing the amplitude with the other two tanks decreases energy according to Fig. 5-(a) and Fig. 5-(b).

However, the situation is reversed when the RF amplitude in the tanks of the ISIS Linac is decreased. In this scenario, Tank 4 exhibits lower energy variation effects and has the least impact on beam transmission efficiency.

With the change of phase in each of the tanks, we have regular behaviour in the output energy of the beam with respect to field amplitude according to Fig. 5-(C) and Fig. 5-(d). By  $+1^\circ$  phase change with respect to nominal operation phase of  $30^\circ$ , the beam energy increased and decreased with the  $-1^\circ$  phase change similarly for all of tanks. In the next section, we will conduct studies on the machine parameters, focusing on the matched input beam, which is pertinent to the machine upgrade involving the MEBT section.

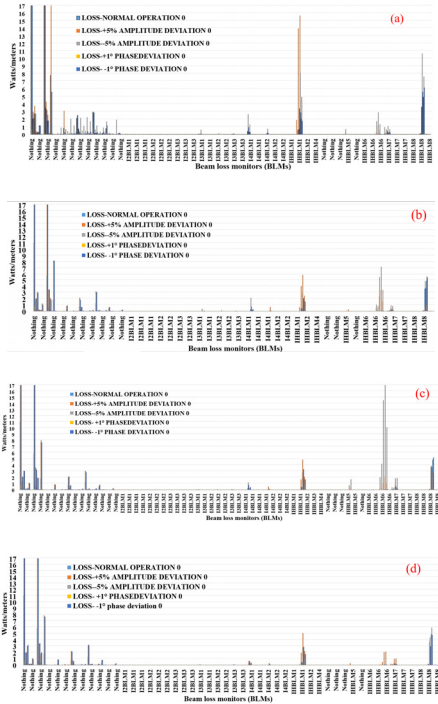


Figure 3: Beam Loss along Linac and HEDS due to phase and amplitude errors in (a) Tank 1, (b) Tank 2, (c) Tank 3, (d) Tank 4.

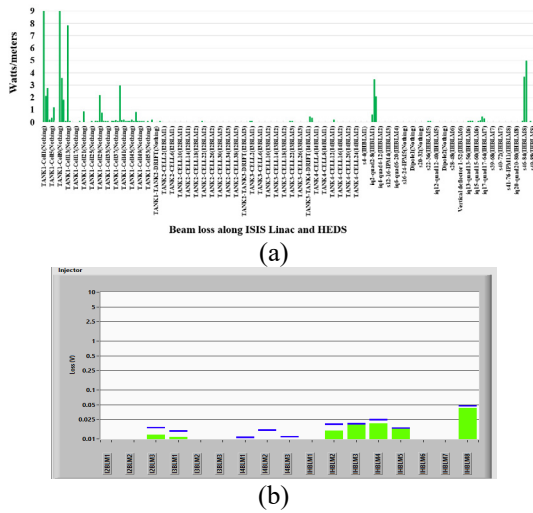


Figure 4: Beam loss along the ISIS injector: (a) estimate of power loss per unit length from simulation with nominal parameters; (b) machine measurement with BLMs.

*(b) ISIS Injector with MEBT*

At the case of completely matched input proton beam, the parameters of input beam to ISIS drift tube linac is:

- Horizontal plane (X-X'):  $\alpha_x = -0.359$ ,  $\beta_x = 0.479$  meters/rad,  $\epsilon_x = \epsilon_{rms-unnorm-x} = 12.7 \pi$ .mm-mrad
- Vertical plane (Y-Y'):  $\alpha_y = -0.188$ ,  $\beta_y = 0.117$  meters/rad,  $\epsilon_y = \epsilon_{rms-unnorm-y} = 12.7 \pi$ .mm-mrad

- Longitudinal plane (W-Phase):  $\alpha_z = -0.127$ ,  $\beta_z = 0.957$  deg/keV,  $\epsilon_z = \epsilon_{rms-unnorm-z} = 120 \pi$ .deg-keV

Operating the linac with a safety margin of 85% to 90% of the RF triode's maximum power is recommended for safe operation. For reference, the required RF power for tanks at different beam currents is represented in Fig. 6.

When dealing with a matched beam and maintaining a phase advance lower than  $90^\circ$ , it is noted that the beam transmission becomes approximately independent of the beam current, and the space charge effect is effectively suppressed. However, it is important to consider that the variations in emittance are more pronounced in the first tank compared to the others. Therefore, ensuring the stability, reliability, and operational performance of the first tank is of paramount importance.

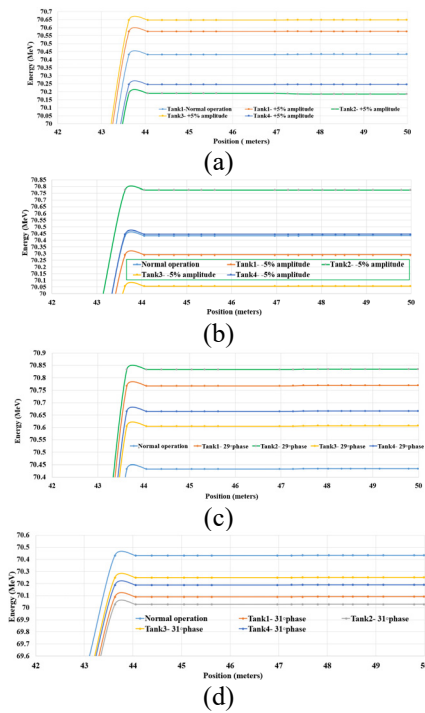


Figure 5: Energy Variation at the end of ISIS linac based on amplitude and phase variation in each of Tanks (a) +5% amplitude, (b) -5% amplitude, (c) +1° phase, (d) -1° phase.

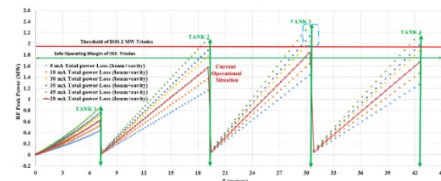


Figure 6: RF power consumption along the cavity length, including cavity loss and beam power.

As depicted in Fig. 7 for various beam currents, it is evident that at these specific beam currents, the horizontal, vertical, and longitudinal emittances experience increases compared to the emittance at zero current, with factors of 2.25, 2, and 2.5, respectively. Despite these emittance variations, the transmission efficiency remains remarkably

Content from this work may be used under the terms of the CC-BY-4.0 licence (© 2023). Any distribution of this work must maintain attribution to the author(s), title of the work, publisher, and DOI

high, surpassing 99.9% for beam currents of 30 and 35 mA. This emphasizes the effectiveness of the MEBT section in maintaining beam transmission at these levels. For a comprehensive view of beam transmission across a range of 0 to 55 mA, please refer to Fig. 8.

Adding the MEBT section between the RFQ and DTL is a significant step, and during the commissioning phase, alignment becomes a critical consideration. Necessary assessments for the displacement and tilt of the input beam in transverse planes have been conducted. When the displacement is kept within 2 mm, the transmission efficiency remains high, exceeding 98%. However, this efficiency drops significantly to 91% when the displacement increases to 3 mm. Notably, the displacement in the y-direction has a more pronounced effect than in the x-direction, as illustrated in Fig. 9(a).

In addition to displacement, introducing a tilt of up to 0.02 radians in the input beam leads to a notable reduction in transmission, particularly for tilt in the x-direction. The alignment of the beam plane is crucial during the adjustment of beam direction, and it becomes even more critical to employ beam position monitors along the length of the MEBT for precise control of beam alignment, as depicted in Fig. 9(b).

Considering a combination of misalignments in both x and y planes, the optimal values for controlling displacement and tilt are less than 0.1 cm and 0.01 radians. Under these conditions, as shown in Fig. 9(c), the transmission efficiency remains high, surpassing 97.7%.

With the current configurations of the MEBT, DTL and HEDS, a milestone has been achieved in maintaining a consistent transmission efficiency along the entire length of the machine, spanning from the RFQ to the RCS. Our transmission efficiency consistently exceeds 99.5%.

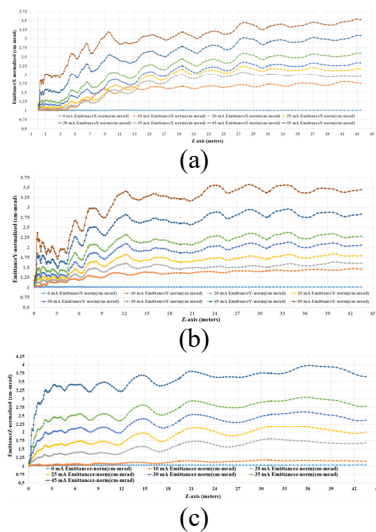


Figure 7: normalized emittances with a matched input beam (a) horizontal, (b) vertical, (c) longitudinal.

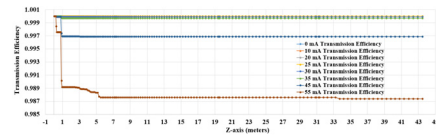


Figure 8: Transmission efficiency of ISIS DTL linac for different input beam currents.

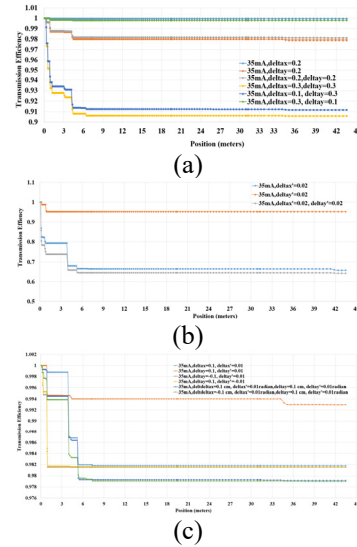


Figure 9: Transmission efficiency for matched input H-beam (a) displacement in X, Y; (b) tilt in X, Y; (c) combinations of displacement and tilt in X, Y.

## CONCLUSIONS

In our study, we conducted comprehensive beam dynamic modelling of the current ISIS linac, achieving a good congruence between our beam loss calculations and experimental measurements. Additionally, we delved into the intricate effects of amplitude and phase variations, recognized as significant contributors to system failures, and dutifully presented the outcomes of our simulations.

Anticipating the forthcoming implementation of the new MEBT system, the consequences of beam misalignment on the linac's transmission was evaluated. Consequently, simulations were performed, confirming that maintaining displacements below 0.1 cm and tilts below 0.01 radians serves as prudent safety margins for optimal performance.

It is noteworthy that once the input beam is matched, transmission becomes nearly impervious to the fluctuations in beam currents.

## ACKNOWLEDGEMENT

We extend our heartfelt gratitude to our esteemed colleagues in the Low Energy Beam and Accelerator Physics groups for their invaluable contributions.

We would also like to express our deep appreciation to the dedicated staff in the control room. Their pivotal role in ensuring the reliability and smooth operation of the machine facilitating our experiments and research, has been truly commendable. It is their diligence that keeps our accelerator system running seamlessly.

## REFERENCES

- [1] A. P. Letchford *et al.*, “Testing, Installation, Commissioning and First Operation of the ISIS RFQ Pre-Injector Upgrade”, in *Proc. PAC’05*, Knoxville, TN, USA, May 2005, paper ROPC010, pp. 695-697.
- [2] S. R. Lawrie *et al.*, “The Pre-Injector Upgrade for the ISIS H-Linac”, in *Proc. LINAC’22*, Liverpool, UK, Aug.-Sep. 2022, pp. 398-401.  
doi:10.18429/JACoW-LINAC2022-TUPOJ021.
- [3] Private communication with H. V. C., 2023.
- [4] S. R. Lawrie *et al.*, “A pre-injector upgrade for ISIS, including a medium energy beam transport line and an RF-driven H<sup>-</sup> ion source”, *Rev. Sci. Instrum.*, vol. 90, p. 103310, 2019. doi:10.1063/1.5127263
- [5] B. Pine, “Space charge induced beam loss on a high intensity proton synchrotron”, PhD thesis, University of Oxford, Oxford, UK, 2016.
- [6] G. P. Boicourt, “PARMILA—An overview”, *AIP Conf. Proc.*, vol. 177, pp. 1-21, 1988.  
doi:10.1063/1.37794
- [7] D. Findlay *et al.*, “Practical guide to the ISIS neutron and Muon Source”, STFC, RAL, ISIS, 2004.
- [8] C. Plostinar *et al.*, “Modelling the ISIS 70 MeV linac”, in *Proc. IPAC’12*, New Orleans, LA, USA, May 2012, paper THPPP052, pp. 3859-3861.
- [9] M. Chimura, H. Harada, and M. Kinsho. “Beam emittance growth due to the strong space-charge field at low energy of a high-intensity ion linac and its mitigation using an octupole magnetic field”, *Prog. Theor. Exp. Phys.*, vol. 2022, no. 6, p. 063G01, 2022.  
doi:10.1093/ptep/ptac077